REPORT DOCUMENTATION PAGE

Form Approved
OMB No. 0704-0188

1. REPORT DATE *(DD-MM-YYYY)*	**2. REPORT TYPE**	**3. DATES COVERED** *(From - To)*
23-05-2006	Technical Paper	

4. TITLE AND SUBTITLE

Plume Characteristics of the Busek 600 W Hall Thruster (Postprint)

5a. CONTRACT NUMBER

5b. GRANT NUMBER

5c. PROGRAM ELEMENT NUMBER

6. AUTHOR(S)

Jared M. Ekholm, William A. Hargus, Jr., & C. William Larson (AFRL/PRSS); Michael Nakles & Garrett Reed (ERC); Carrie S. Niemela (Spiral Technology)

5d. PROJECT NUMBER
10110011

5e. TASK NUMBER

5f. WORK UNIT NUMBER

7. PERFORMING ORGANIZATION NAME(S) AND ADDRESS(ES)

Air Force Research Laboratory (AFMC)
AFRL/PRSS
1 Ara Drive
Edwards AFB CA 93524-7013

8. PERFORMING ORGANIZATION REPORT NUMBER

AFRL-PR-ED-TP-2006-156

9. SPONSORING / MONITORING AGENCY NAME(S) AND ADDRESS(ES)

Air Force Research Laboratory (AFMC)
AFRL/PRS
5 Pollux Drive
Edwards AFB CA 93524-70448

10. SPONSOR/MONITOR'S ACRONYM(S)

11. SPONSOR/MONITOR'S NUMBER(S)
AFRL-PR-ED-TP-2006-156

12. DISTRIBUTION / AVAILABILITY STATEMENT

Approved for public release; distribution unlimited (AFRL-ERS-PAS-2006-114)

13. SUPPLEMENTARY NOTES

 Presented at the 42nd AIAA/ASME/SAE/ASEE Joint Propulsion Conference, Sacramento, CA, 9-12 July 2006. AIAA 2006-4659.

14. ABSTRACT

To better characterize the potential impacts of the operation of a Busek Company, Inc. BHT-HD-600 laboratory Hall thruster on spacecraft, a number of plume properties have been measured. These include current density using a Faraday probe, ion energy distribution using a retarding potential analyzer, and ion species fractions using an E x B probe. The BHT-HD-600 Hall thruster is a nominally 600 W xenon Hall thruster developed by Busek Co. Inc. for the U.S. Air Force Research Laboratory. Plume characterization of Hall thrusters is required to fully understand the impacts of thruster operation on spacecraft. Much of these plume data are vital inputs for numerical models that can then be applied to estimate the effect of the energetic plume on complex spacecraft geometries. Early measurement of plume properties, such as plume divergence, ion energy distribution, and species fractions, aids the timely transfer of Hall thruster technology to the user. The plume's ion beam was characterized by measurement of ion current density radial profiles, ion energy spectra and ion species fraction distributions. Measurements were recorded ±90° off thruster centerline at 60 cm from the discharge. It was determined slight variations in anode potential and mass-flow produced a measurable effect on ion current density and plume divergence, experimentally showing an increase or decrease of ±15-20%. Ionic energy spectra demonstrated both inelastic and elastic scattering within the plume. The measurements reveal significant populations of multiply-charged ions in the plume. E x B probe measurements show surprisingly ion species fraction angle dependence.

15. SUBJECT TERMS

16. SECURITY CLASSIFICATION OF:			**17. LIMITATION OF ABSTRACT**	**18. NUMBER OF PAGES**	**19a. NAME OF RESPONSIBLE PERSON**
					Dr. William A. Hargus, Jr.
a. REPORT	**b. ABSTRACT**	**c. THIS PAGE**	A	11	**19b. TELEPHONE NUMBER** *(include area code)*
Unclassified	**Unclassified**	**Unclassified**			N/A

42nd AIAA/ASME/SAE/ASEE Joint Propulsion Conference & Exhibit
9 - 12 July 2006, Sacramento, California

AIAA 2006-4659

Plume Characteristics of the Busek 600 W Hall Thruster

Jared M. Ekholm*, William A. Hargus†, C. William Larson‡
Air Force Research Laboratory, Edwards Air Force Base, CA, 93524
Michael R. Nakles§, Garrett Reed¶
ERC, Inc., Edwards Air Force Base, CA, 93524
Carrie S. Niemela‖
Spiral, Inc. Edwards Air Force Base, CA, 93524

To better characterize the potential impacts on a spacecraft during operation of a Busek Company, Inc. BHT-HD-600 laboratory Hall thruster, a number of plume properties have been measured. These measurements include current density using a Faraday probe, ion energy distribution using a retarding potential analyzer and ion species fractions using an E×B probe. Developed by Busek Co., Inc. for the U.S. Air Force Research Laboratory, the BHT-HD-600 Hall thruster is a nominally 600 W xenon Hall thruster. Plume characterization of Hall thrusters is required to fully understand the impacts of thruster operation on spacecraft. Much of these plume data are vital inputs for numerical models that can then be applied to estimate the effect of the energetic plume on complex spacecraft geometries. Early measurement of plume properties, such as plume divergence, ion energy distribution and species fractions, aids the timely transfer of Hall thruster technology to the user. The plume's ion beam was characterized by measurement of ion current density radial profiles, ionic energy spectra and ion species fraction distributions. Measurements were recorded $\pm 90^{\circ}$ off thruster centerline at 60 cm from the discharge. It was determined slight variations in anode potential and mass-flow produced a measurable effect on ion current density and plume divergence, experimentally showing an increase or decrease of $15-20\%$. Ionic energy spectra demonstrated both inelastic and elastic scattering within the plume. The measurements reveal significant populations of multiply-charged ions in the plume. E×B probe measurements show surprisingly ion species fraction angle dependence.

I. Introduction

Hall thrusters are an ideal propulsion technology for numerous spacecraft missions including orbit raising, orbit transfers, as well as station keeping due to their relatively high specific impulse and thrust densities. The issue of spacecraft integration is highly important as high-energy ions may sputter and erode spacecraft surfaces increasing operational risk. In order to adequately characterize a Hall thruster plume, extensive analysis of the plume is necessary. The goal of this work is to better characterize BHT-HD-600 Hall thruster plume to better understand spacecraft-plume interactions. The BHT-HD-600 Hall thruster, a candidate technology for small satellites with limited power, is a nominally 600 W xenon Hall thruster developed by Busek Co., Inc. for the U.S. Air Force Research Laboratory (AFRL). A number of tests were conducted to investigate plume properties at a number of operating conditions to include ion current density profiles, ionic energy spectrum and ion species fraction distribution. A Faraday probe, retarding potential analyzer (RPA) and an E×B Probe were employed to quantify the plasma plume. This information will then be transferred

*Research Scientist, AFRL/PRSS, 1 Ara Road Edwards AFB, CA 93524, and Member AIAA.
†Research Engineer, AFRL/PRSS, 1 Ara Road Edwards AFB, CA 93524, and Senior Member AIAA.
‡Research Engineer, AFRL/PRSS, 1 Ara Road Edwards AFB, CA 93524, and Member AIAA.
§Research Engineer, AFRL/PRSS, 1 Ara Road Edwards AFB, CA 93524, and Member AIAA.
¶Research Engineer, AFRL/PRSS, 1 Ara Road Edwards AFB, CA 93524, and Member AIAA.
‖Research Engineer, AFRL/PRSS, 1 Ara Road Edwards AFB, CA 93524, and Member AIAA.

to our modeling and simulation group and will be used to generate advanced plasma plume models so that we can determine the effect of the BHT-HD-600 plume on potential spacecraft configurations. This data is therefore necessary to provide seed data to both serve as seed data and to verify the plume models [Niemela et al].

II. Experimental Apparatus

A. Busek BHT-HD-600 Hall Thruster

The Busek BHT-HD-600 Hall thruster originates from Busek's family of high performance Hall thrusters. The thruster shown in Fig. 1 operates at a nominal 600 W generating 36 mN of thrust at an efficiency of 46% while operating at a discharge voltage of 300 V and propellant flow rate of 2.5 mg/sec. Under these operating parameters the anode specific impulse measures 1500 sec [B. Pote Personal Communication]. The analysis in this effort investigates the plume at these nominal conditions as well as the sensitivity of the plume to small discharge and propellant flow variations. During these tests the anode discharge varied from 200 through 350 V at 25 V increments and propellant flow rate 15% off nominal conditions.

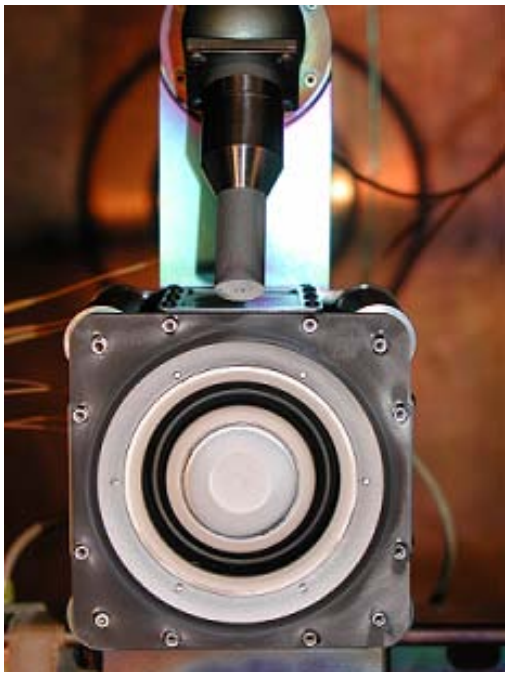

Figure 1. Busek BHT-HD-600 Hall Thruster. ***Busek's 600 W Hall thruster has been identified as a candidate for future microsatellites due to its high performance and modest power consumption.***

B. Nude Faraday Probe

The Faraday probe, shown in Fig. 2, measures ion beam current downstream of the thruster.[1] Xenon ions impacting the collector induce a current, which is then recorded via an ammeter. The collector is 19.1 mm in diameter while the guard ring measures 45 mm with approximately 1.5 mm spacing between. The inner current collector and guard ring were biased to -30 V to ensure ion collection at both surfaces occurs in the ion saturation regime. The purpose of the guard ring is to create a uniform sheath thickness in the collector region by avoiding edge effects in the portion of the probe where the ions are measured. The probe was situated 60 cm from the thruster exit plane, mounted on a rotary translation stage. During measurements, the plume current density was measured from $\pm 90^\circ$ with 5° intervals. Probe currents recorded at highly oblique angles ($\pm 60^\circ$) require special attention due to the presence of charge exchange ions. Ions created in the anode region may collide with slow-moving neutrals resulting in an exchange of an electron, thereby, producing a fast moving neutral and an ion with velocity similar to the originally neutral. This is believed to lead to an increase in measured current especially at oblique plume angles. It is difficult to identify or eliminate this portion of the signal and no correction was made for multiply-charged ions or any other effects of ion impingement on the collector surface.

C. Retarding Potential Analyzer

Using a series of fine biased grids, an RPA filters ions based on energy which can be used to generate an ion energy distribution. The RPA, developed by Haas,[2] used in these measurements consists of three distinct grids separated by insulators. The first grid acts as an aperture and is maintained at the local floating potential. The second grid, biased to -30 V, repels electrons within the plasma while ensuring ions pass through. Finally, the third grid is swept from 0 through 500 V retarding ions based on their energy. While the probe is able to determine the energy, it is only capable of measuring the energy per charge (E/q) distribution. Some ambiguity is created by the presence of multiply-charged ions. Those created within the thruster will be indistinguishable from singly-charged ions since they will have passed through the same potential drop as the majority of the singly-charged ions and will consequently have the same E/q ratio. Ions

created outside the main discharge whether by charge exchange or electron bombardment will have energies that may be different than ions created within the thruster. Identification and complete characterization of these non-standard ion populations is challenging.

Figure 2. Nude Faraday Cup. ***Inner collector and sheath seen in above picture with slight gap between.***

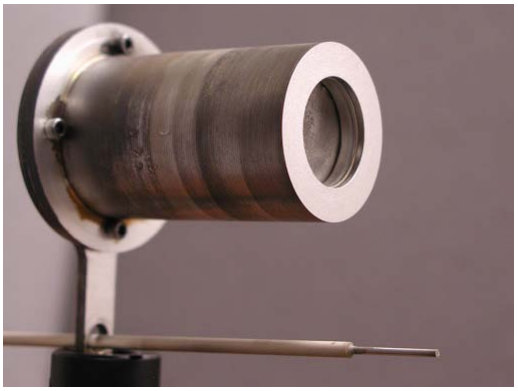

Figure 3. RPA with Langmuir Probe. ***Although the measurements were taken concurrently, the Langmuir probe measurements could not distinguish the electron saturation point.***

D. E×B Probe

The E×B probe uses the Lorentz force to separate ions according to their velocity class. Also known as a Wein filter,[3] the E×B probe utilizes perpendicular electric and magnetic fields to filter the beam by the ion's respective velocity. By the Lorentz equation, only a single velocity class will pass through the E×B probe without being deflected. Hence only the velocity class of interest is passed through the probe collimator and sensed at the ion collector. The E×B probe is constructed of three separate sections: the collimator, E×B field section and the ion collector. The collimator focuses the ions into a beam before entering the E×B test section. Once subjected to the electric and magnetic fields within the test section, ions lacking the correct velocity or energy will be deflected into the walls of the test section and prevented from entering the collimated collector. Two permanent ceramic magnets create the magnetic field generating 0.129 Tesla. The electric field is supplied by two bias plates ramped from 0 through 60 V with an effective upper limit of ion species energy of 1500 eV (Xe). The geometry of the grounded collector is optimized to collect any generated secondary electrons thereby maximizing current collection. The current is then measured on a pico-ammeter through a shielded coaxial cable.

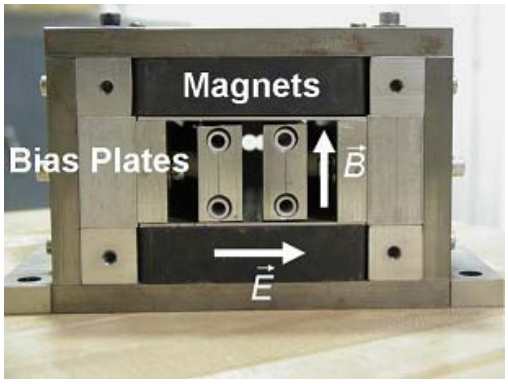

Figure 4. E×B Probe. ***Note orientation of magnetic and electric fields within the test section. Front plate has been removed.***

By scanning the electric field, it is possible to generate the velocity profile of the ion stream at a particular plume location; however, the accuracy of the calculated ion velocities and derived ion energies is limited by the accuracy of the alignment of the probe fields and collimation screens. The primary use of the E×B probe is in the identification of various ionic charge states. The E×B probe is able to distinguish between the various ionic species so long as they are created in the same region and pass through the same potential fall. For example those ions created within the Hall thruster where the various ions are all accelerated to the same energy, Vq. However, ions created, or which have modified their charge state in the plume, are more difficult to unambiguously identify.

E. AFRL Chamber 6

All measurements presented in this work were conducted in Chamber 6 at the AFRL Electric Propulsion Laboratory located at Edwards AFB, CA. Chamber 6 measures 1.8 m diameter and 3.0 m length with a pumping speed of 32,000 l/s on xenon using four single stage cryogenic panels and one 50 cm dual stage cryogenic tub-style pump. During operations chamber pressure is approximately 7×10^{-4} Pa, corrected for xenon. The chamber was setup as seen in Figs. 5 and 6. Figure 5 shows the E×B probe experimental set up where the probe, due to its high mass, was fixed and the thruster was rotated. Figure 6 shows the Faraday probe experimental setup (It is nearly identical to the RPA setup.) where the probe was rotated and the thruster was fixed. Due to the chamber geometry, E×B measurements were limited to $-30°$ through $70°$ unlike the Faraday probe and RPA measurements which collected data along a $\pm 90°$ arc.

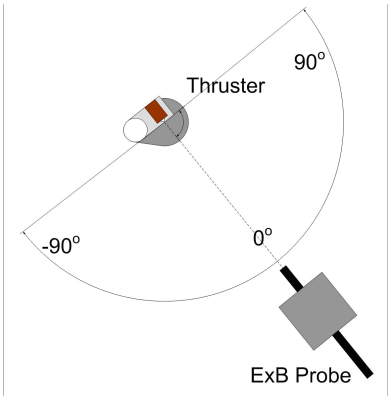

Figure 5. Chamber 6 Setup for E×B Probe Measurements. ***Due to chamber and probe dimensions only angles*** $-30°$ ***through*** $70°$ ***were investigated.***

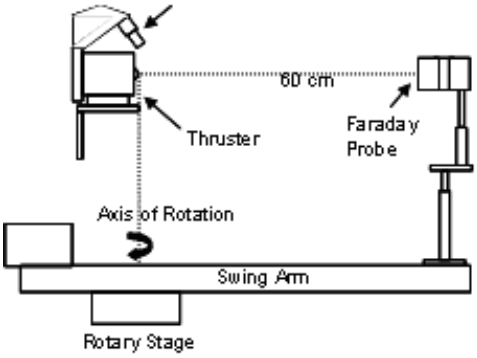

Figure 6. Chamber 6 Setup for Faraday and RPA Measurements. ***Thruster setup was centered on chamber axis achieving scanning capability of*** $\pm 90°$***.***

III. Results and Discussion

A. Ion Beam Current

Ion current flux was measured with the Faraday probe previously described. As shown in Fig. 6, the Faraday probe was mounted on a radial arm, and the probe rotated in an arc 60 cm from the thruster exit plane measuring current density at angles $\pm 90°$ off centerline via a stepper motor driven rotary stage and LabView® data acquisition based system. The anode potential on the thruster was varied between 200 and 350 V in 25 V intervals. Additional testing performed at off-nominal flow rates ($\pm 15\%$), which produced data showing the plume sensitivity to flow rates. During all measurements the collector was biased to -30 V to ensure the collector remained in the ion saturation regime. Typical current densities measured 14 A/m^2 at $0°$ and nominal operating conditions. Higher current densities were measured at increased flow rates and elevated discharge voltages as well as lower values at reduced mass-flow rates and discharge potentials.

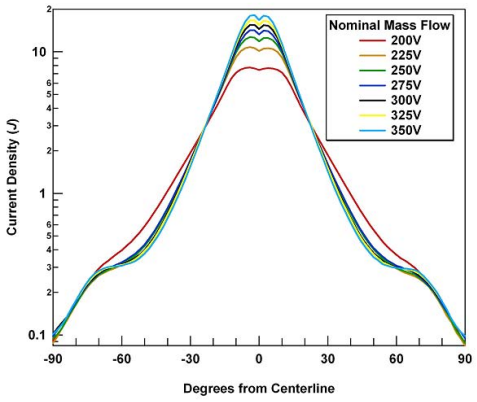

Figure 7. Faraday Cup Measurements. ***Note presence of plume wings at angles*** $\pm 60°$

Faraday probe traces for the nominal propellant flow rate are shown in Fig. 7 and depict the relationship between discharge potential and current density. Increasing anode potential results in increasing central current density. Common to Faraday probe measurements on many Hall thrusters, the traces showed similar properties with maximum current density located at $\pm 5°$ off thruster centerline and a dip at $0°$ presumably reflecting the annular discharge geometry. The presence of charge exchange ions can be inferred to be responsible for

at least a portion of the wing structure evident in Fig. 7. The presence of charge exchange ions in this region are attributed to the vacuum chamber background pressure of neutral xenon.[4,5] Along the thruster centerline, the relative population of charge exchange ions is small in comparison to ions formed within the anode discharge. Meanwhile at large angles, the relative population of charge exchange ions increases due to the increased divergence of charge exchange populations.

The source and energies of the plume produced charge exchange ions may be explained by noting the thruster geometry. Primary ions produced within the discharge cavity have no direct path to the oblique angles and can only be routed there through collisions or radial acceleration by electric forces generated by a negatively biased chamber or satellite surfaces. Therefore it is believed that multiply-charged ions produced within the discharge will most likely be accelerated along the same paths as singly-charged primary ions. However as chamber backpressure increases, additional neutrals are present increasing the probability of collisions. Both momentum exchange and charge exchange collision cross-sections are of similar magnitude. With the increased probability of collisions and the charge exchange population increasing in the plume, the Faraday probe collects these ions in addition to the primary ions artificially increasing the measured current especially in the wings where they are most evident.[6]

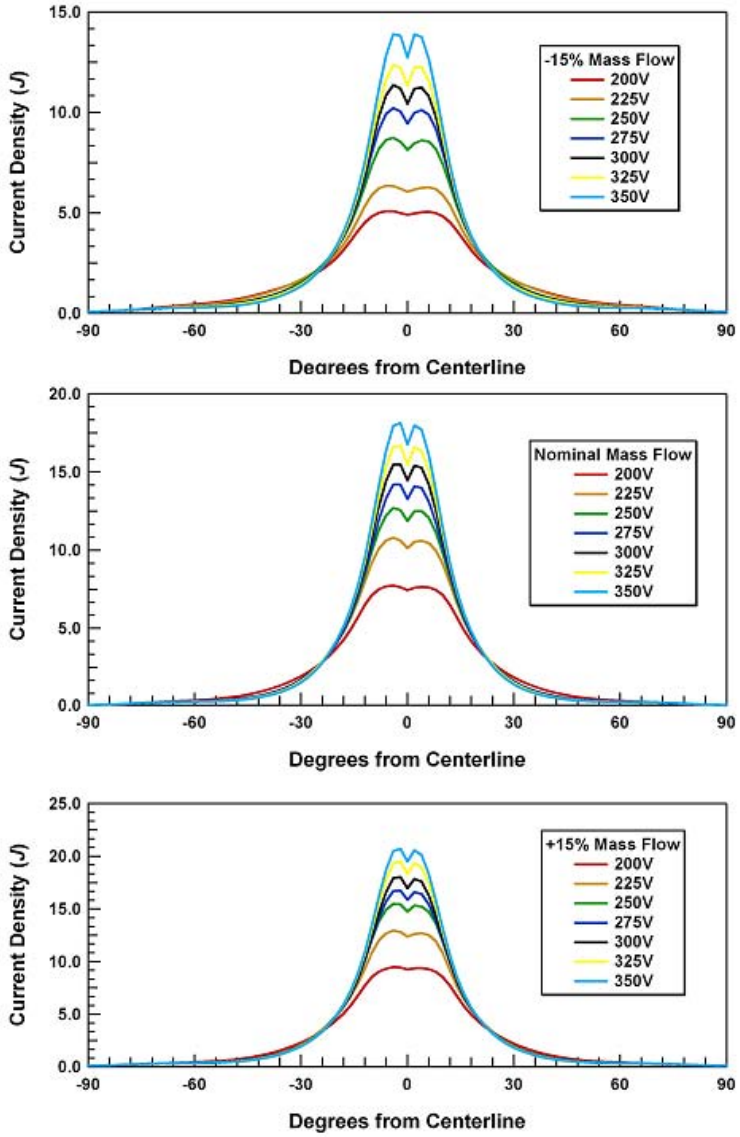

Figure 8. Current Density (J) and Mass-Flow Relationships. ***Faraday probe traces*** -15%**,** ***nominal and*** $+15\%$**.**

Figure 8 illustrates the effects on current density as the mass-flow varies ±15% off nominal conditions over a range of anode potentials. As expected, current density increases as a function of mass-flow rate. Decreased flow rates of −15° yield a current density of 70% of nominal flow due to the reduced Xe neutral density within the discharge chamber. Whereas flow rates of +15% result in a current density 120% of optimal operating parameters due to the increased propellant flow. Additionally, the peak current density increases as a function of increasing discharge voltage as the current density profile itself narrows. At 200 V, the peak current density is 50% of nominal, and at 350 V, it measures 115% of nominal. It should also be noted that due to the fixed pumping speed of the vacuum facility, the background pressure during these tests is proportional to the mass-flow rate. Consequently, the likelihood of collisions with background neutral Xe increases which increases the number of charge exchange and momentum exchange collisions.

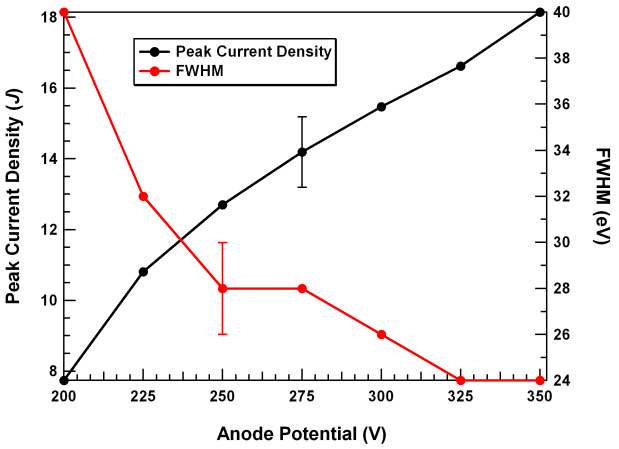

Figure 9. Peak Current Density and FWHM. ***Note inverse relationship on plume broadening with increasing anode potential and current density at nominal mass flow rates.***

By altering the thruster operating parameters, the plume divergence can be varied to some degree. Faraday probe measurements provide a method of analyzing plume divergence as the operating conditions are changed. By examining the full width at half maximum (FWHM) insights into plume divergence can be inferred. Figure 9 shows the dependency of the plume profile width (characterized as FWHM) as a function of anode potential as well as the behavior of the peak current density at nominal flow rates. It shows clearly that as the discharge potential is increased, the profile narrows and the peak current density rises.

B. Ionic Energy Distribution

Ionic energy distribution data was gathered using an RPA mounted on an apparatus identical to that used for the Faraday probe measurements previously discussed. An RPA potential sweep from 0 through 500 V sufficiently filtered ions according to their respective energy across the spectrum. Figure 10 shows a matrix of area normalized distribution functions ±90° with 30° increments from thruster centerline for several anode potentials. The measurements display symmetry between one another denoting good alignment and repeatability in the measurements. As oblique plume angles identified to be in the wings of the current density measurements were probed, a secondary peak emerged. This first became apparent at ±60° with energy of approximately 50 V. This peak corresponds to a reducing primary-to-charge exchange ion ratio as a function of increasing angle.[6] Moving further from thruster centerline, the dominance of the secondary peak at ±90° illustrates another mechanism for particle acceleration outside the main discharge chamber.

Table 1. Full Width at Half Maximum. ***Recorded along thruster centerline at nominal propellant flow.***

Anode Potential	FWHM (eV/q)
200	44.25
225	44.24
250	45.88
275	54.08
300	75.39

In addition to charge exchange collisions, the plume outside of the main discharge beam consists of elastically scattered ions as demonstrated by Mikellides and Katz.[7] Within the near-field region, the high-energy ions created within the chamber undergo elastic scattering with a large population of neutrals exhausted from the thruster. At different angles, one mechanism will dominate over another and account for certain energy peaks. In addition, they demonstrated the emergence of this energy peak at oblique angles denotes an energy dependence on angle, which closely follows $E_L cos^2\Psi$ where E_L represents the main beam ion energy and Ψ, the angle from centerline. The same energy-angle relationship appears to occur in this case.

As would be expected, ionic energy increases with anode potential. As more potential is applied to the discharge, the ions experience a greater accelerating force, resulting in higher velocities, and thus kinetic

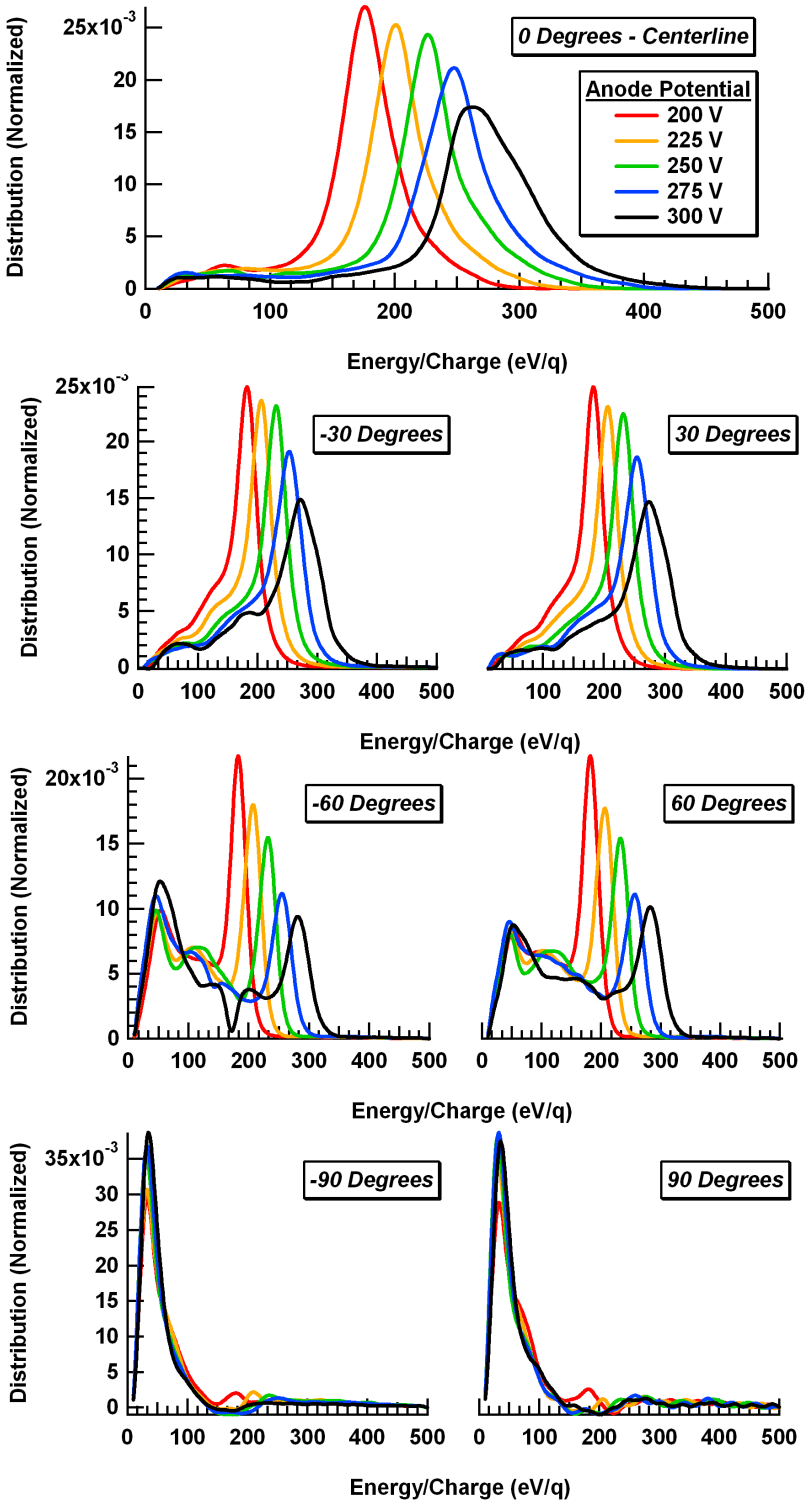

Figure 10. Energy Distribution Measurements. *The increased ion scattering can be seen as the secondary peak becomes more prominent further away from centerline. Note symmetry agreement between measurements.*

energy. In addition to the increase in kinetic energy, broadening of the energy distribution increases as anode potential increases. Table 1 shows the anode potential in comparison with the ionic energy profile width (FWHM), where the anode potential varies between 200 and 350 V. By varying the anode potential, the ionic energy distribution effective narrows by only 4% at 200 V, yet at 300 V broadens by 64% when compared to nominal operating conditions (300 V). Interestingly, reduced discharge potentials have little, or no, effect on the ionic energy profile width whereas elevated anode potentials dramatically increased the ionic energy profile.

Figure 11 depicts ionic energy distribution area normalized peak signal strength with respect to plume angle from centerline, $\pm 90°$ in $30°$ increments. All traces follow similar patterns with minimums found at $\pm 60°$. Maximum ion energies were recorded at the highly oblique angles of the plume, $> \pm 90°$. Nearly all traces exhibit a localized peak at thruster centerline. A rapid increase in ionic energy peak magnitude beyond $60°$ occurs in the same region in which charge exchange ions were measured with the Faraday probe. Increasing anode potentials result in a wider distribution profiles rather than reduced anode potentials.

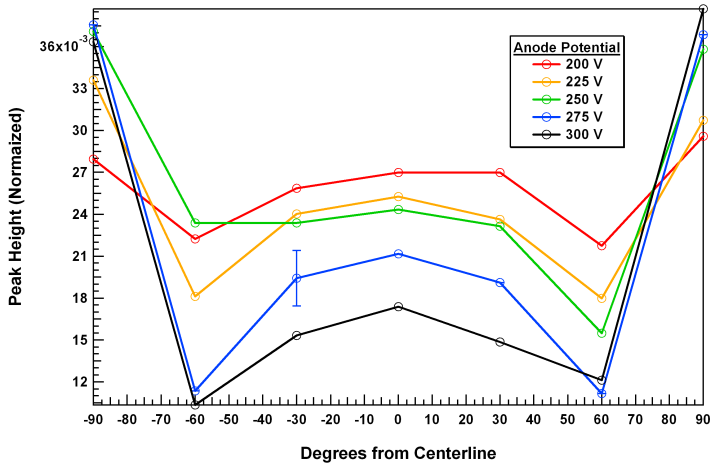

Figure 11. Ion Energy Peak Magnitude Relationship to Plume Angle. ***Note the rapidly increasing signal strength at the highly oblique angles,*** $> \pm 60°$ ***from thruster centerline.***

C. Ion Species Fractions

The ion species distributions of the plume were determined using the E×B probe. The probe was located 60 cm from the thruster on a stationary pedestal. Due to the low weight of the thruster relative to the heavy iron E×B probe and due to the limited diameter of the chamber, the thruster was rotated while the probe remained stationary. This allowed for the E×B probe to sample the plume between $-30°$ and $+70°$.

Figure 12 shows a typical trace with the measured current as a function of calculated energy from 0 to 1550 eV. Three distinct peaks were observed indicating the presence of Xe^{+1}, Xe^{+2} and Xe^{+3} species within the plume. Xe^{+4} was detected in some of the traces, yet its respective ion species fraction was not sufficiently resolved to within calculated reliable fractions in these measurements. Signal magnitudes were less than 5×10^{-10} A on centerline for nominal conditions, and as expected signal decreased with increasing angle due to reduced ion flux. Although, signal strength was more than adequate, the calculated energy of the ions was unrealistically low and does not correspond well to our other measurements. Previous E×B probe measurement on a 200 W Hall thruster produced good agreement with established values,[3] yet when the 600 W Hall thruster was probed, measurements yielded lower than expected energies. The discrepancy in energies was repeatable in

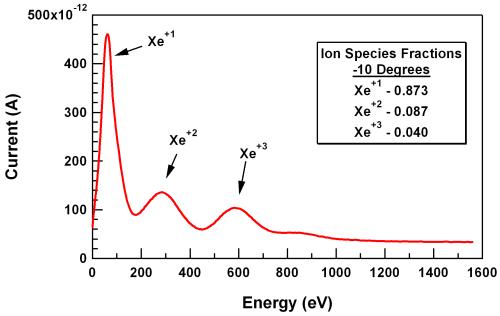

Figure 12. Typical E×B Trace. ***Note distinct peaks for three ion species indication the presence of*** Xe^{+1}, Xe^{+2} ***and*** Xe^{+3}. ***Note: calculated energy values are incorrect.***

each iteration. The singly-charged peak was recorded at 50 eV, doubly-charged at 280 eV and triply-charged at 590 eV, substantially off expected values.

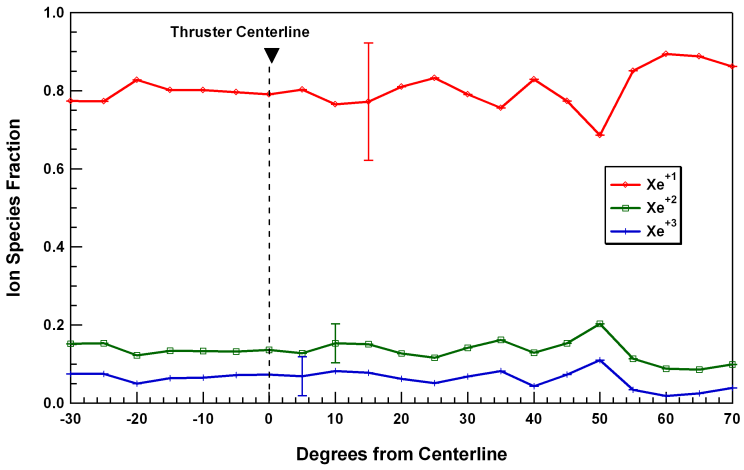

Figure 13. Ion Species Trends. ***Note relative consistency of ion species fraction measurements throughout the plume.***

The disagreement in results may be due to a misalignment of the probe collimator or to temperature variations which modified the magnetic field (B). Although the thermal mass of the probe measures 20.5 kg, the magnets may be substantially heated by the ion beam, altering the strength and uniformity of the magnetic field. If so, the collected current would not correspond to the calculations of the magnetic field outside of the chamber. Multiple measurements on the magnetic field were recorded upon removal of the probe from the chamber. Each instance the geometry and the strength of the magnetic field remained constant. Future tests will include installation of thermocouples to the E×B probe so the temperature deviation may be recorded during testing.

Despite the incorrect calculated ion energies, the data still allowed for the calculation of the relative species fractions. In all portions of the plume, the ion species fraction distribution remained relatively uniform with slight variations beyond 50° as shown in Fig. 13. This result was not consistent with previous 200 W results which showed Xe^{+1} population maximums along thruster center and minimums at highly oblique angles, 60°. Additionally, BHT-200 results showed multiply-charged ions experienced a minimum at 0° and maximums in the oblique angles in the 200 W plume.[3]

IV. Conclusions

This effort investigated the plume characteristics of a Busek BHT-HD-600 Hall thruster. Examining the plasma characteristics at varying operating conditions provides insight the sensitively of the plume properties to the operating conditions. Several factors including the production of multiply-charged xenon ion species have adverse effects on spacecraft operations and these effects must be further characterized. Faraday probe measurements confirm ion current density increases with both anode potential and mass flow. Increases of 120% are seen under increased operating parameters while, decreases in propellant flow and anode potential result in current densities of 50% and 60% of nominal. The plume broadens with increasing anode potential as shown by the FWHM of the respective traces. Both momentum exchange and charge exchange collisions appear to be occurring within the plume. These result in low energy ions entering the wings in the oblique plume. These ions will require greater examination as they are a likely source of ions which will interact with a spacecraft. Species fraction measurements taken using the E×B probe showed a flat distribution of multiply-charged ions with little angular variation. These results will be incorporated into numerical models and be presented in the future.

V. Acknowledgements

The authors would like to thank Bruce Pote and Larry Byrne of Busek Co., Inc. for their efforts in support of these measurements as well as Richard R. Hofer and Lee Johnson of the Jet Propulsion Laboratory for their contributions in understanding the low-energy ion populations at highly oblique plume angles.

References

[1]Hargus Jr., W. A. and Straffacia, J., "Optical Boron Nitride Insulator Erosion Characterization of a 200 W Xenon Hall Thruster," *41st Joint Propulsion Conference*, Tucson, AZ, 2005, AIAA-2005-3529.

[2]Hofer, R. R. and Haas, J., "Ion Voltage Diagnostics in the Far-Field Plume of a High-Specific Impulse Hall Thruster," *39th Joint Propulsion Conference*, Huntsville, AL, 2003, AIAA-2003-4556.

[3]Ekholm, J. M. and Hargus Jr., W. A., "Ion Species Fractions of a 200 W Hall Thruster," *41th Joint Propulsion Conference*, Tucson, AZ, 2005, AIAA-2005-4405.

[4]de Grys, K. H., Tilley, D. L., and Aadland, R. S., "BPT Hall Thruster Plume Characteristics," *35th Joint Propulsion Conference*, Los Angeles, CA, 1999, AIAA-1999-2283.

[5]Walker, M. L., Victor, A. L., Hofer, R. R., and Gallimore, A. D., "Effect of Backpressrue on Ion Current Density Measurements in Hall Thruster Plumes," *Journal of Propulsion and Power*, Vol. 21, No. 3, 2005, pp. 408–415.

[6]Beal, B., *Clustering of Hall Effect Thrusters For High-Power Electric Propulsion Applications*, Ph.D. thesis, University of Michigan, Ann Arbor, MI, 2003.

[7]Mikellides, I. G., Katz, I., Kuharshi, R. A., and Mandell, J., "Elastic Scattering of Ions in Electrostatic Thruster Plumes," *Journal of Propulsion and Power*, Vol. 21, No. 1, 2005.